polysaccharides

MDPI

Article

Preservation of Rabbit Meat in High-Density Polyethylene Packaging Bags Reinforced with Ethyl Cellulose Nanoparticles Loaded with Rosemary Extract

Brenda Sánchez-Camacho [1], María de la Luz Zambrano-Zaragoza [2,*], José Eleazar Aguilar-Toalá [3], Rosy Gabriela Cruz-Monterrosa [3], Monzerrat Rosas-Espejel [3] and Jorge L. Mejía-Méndez [4]

[1] División de Ciencias Biológicas y de la Salud, Universidad Autónoma Metropolitana, Unidad Lerma (UAML), Av. de las Garzas 10, Col. El Panteón, Lerma de Villada 52005, Mexico; 2193039353@correo.ler.uam.mx
[2] Laboratorio de Procesos de Transformación y Tecnologías Emergentes de Alimentos, FES-Cuautitlán, Universidad Nacional Autónoma de México, Cuautitlán Izcalli 54714, Estado de México, Mexico
[3] Departamento de Ciencias de la Alimentación, División de Ciencias Biológicas y de la Salud, Universidad Autónoma Metropolitana, Unidad Lerma (UAML), Av. de las Garzas 10, Col. El Panteón, Lerma de Villada 52005, Mexico; j.aguilar@correo.ler.uam.mx (J.E.A.-T.); r.cruz@correo.ler.uam.mx (R.G.C.-M.); m.rosas@correo.ler.uam.mx (M.R.-E.)
[4] Programa de Edafología, Colegio de Postgraduados, Campus Montecillo, Carr. México Texcoco km 36.5, Montecillo 56264, Mexico; mejia.jorge@colpos.mx
* Correspondence: luz.zambrano@unam.mx

Abstract

In this work, ethyl cellulose nanoparticles loaded with rosemary extract (RCL-NPs) were synthesized and utilized to reinforce high-density polyethylene (HDPE) packaging bags as a nanotechnological alternative for rabbit meat preservation. The synthesized RCL-NPs were characterized by DLS and for their stability. The analyzed variables of rabbit meat packaged samples included drained liquid, weight loss, color, pH, texture, and hardness. The total phenolic content (TPC) and antioxidant capacity of rosemary extract were also investigated. The results demonstrated that RCL-NPs were 117.30 nm in size with a negative surface charge (−24.59 mV) and low PDI (0.12). According to the Higuchi model, the release rate of RCL-NPs was sustained from 0 to 24 h. The encapsulation efficiency of the implemented synthesis route was 99.97%. The TPC of rosemary extract was 566.13 ± 1.72 mg GAE/L, whereas their antioxidant activity utilizing the DPPH and FRAP assays was 27.86 ± 0.32 mM Trolox/L and 0.31 mM Trolox/L, respectively. Contrary to control samples, rabbit meat samples conserved in HDPE packaging bags reinforced with RCL-NPs prevent drained liquid and weight loss, while preserving *L (60 ± 2.5–66.10 ± 2.0) and *b (10.67 ± 2.28–11.62 ± 2.39), pH (5.22 ± 0.05–5.80 ± 0.03), and texture (10.37 ± 0.82–0.70 ± 0.50). In the same regard, the developed material conserved the hardness of rabbit meat samples, exhibiting values that ranged from 27.79 ± 7.23 to 27.60 ± 3.05 N during the evaluated period (0–13 days). The retrieved data demonstrate the efficacy of RCL in preserving the quality of rabbit meat when integrated with additional food packaging materials.

Keywords: nanotechnology; food packaging; rabbit meat; ethyl cellulose nanoparticles; rosemary extract

check for updates

Academic Editor: Cédric Delattre

Received: 15 June 2025
Revised: 23 July 2025
Accepted: 28 August 2025
Published: 29 August 2025

Citation: Sánchez-Camacho, B.; de la Luz Zambrano-Zaragoza, M.; Aguilar-Toalá, J.E.; Cruz-Monterrosa, R.G.; Rosas-Espejel, M.; Mejía-Méndez, J.L. Preservation of Rabbit Meat in High-Density Polyethylene Packaging Bags Reinforced with Ethyl Cellulose Nanoparticles Loaded with Rosemary Extract. *Polysaccharides* **2025**, *6*, 76. https://doi.org/10.3390/polysaccharides6030076

Copyright: © 2025 by the authors. Licensee MDPI, Basel, Switzerland. This article is an open access article distributed under the terms and conditions of the Creative Commons Attribution (CC BY) license (https://creativecommons.org/licenses/by/4.0/).

1. Introduction

Rabbit meat offers a lean and nutritious protein source with several culinary applications. It is low in fat and cholesterol while being rich in essential amino acids, vita-

mins, and minerals. Geographically, the consumption of rabbit meat varies significantly among countries, Asia and America being the regions with the highest global rabbit meat production [1]. Common materials used in rabbit meat packaging include plastics (e.g., polyethylene, polypropylene, and polyethylene terephthalate), metals (e.g., aluminum and tinplate), glass, and paper-based products [2–4]. High-density polyethylene (HDPE) is a thermoplastic polymer composed of propylene monomers. Physicochemically, HDPE has a semi-crystalline structure with high density (0.94–0.97 g/cm^3), and it is inert and resistant to many solvents. Oppositely to other packaging materials, HDPE provides an effective oxygen barrier to prevent oxidation and maintains the moisture content of meat products. Additionally, it can be heat-sealed for airtight packaging and is transparent, allowing visual inspection of meat quality [5].

Nanotechnology involves manipulating matter at the nanoscale, typically ranging from 1 to 100 nanometers. This field encompasses the design, production, and application of materials and devices at this scale. Synthesis methods for nanomaterials (NMs) encompass both top-down approaches, such as mechanical milling, lithography, and laser ablation, as well as bottom-up approaches, including chemical vapor deposition, sol–gel processing, and self-assembly [6]. Common types of NMs include carbon-based materials [7], metal-based nanoparticles, dendrimers [8], quantum dots [9], and nanocomposites such as the integration of nanoparticles (NPs) with bulk materials.

Ethyl cellulose is a naturally occurring polysaccharide composed of β-D-glucose units linked by β(1→4) glycosidic bonds, forming a linear, fibrous structure [10]. Contrary to other polysaccharides, ethyl cellulose is considered the most abundant organic polymer on Earth, serving as the primary structural component of plant cell walls. Physically, ethyl cellulose is characterized by its high tensile strength, crystallinity, and insolubility in water and most organic solvents, due to extensive intra- and intermolecular hydrogen bonding [11]. Chemically, ethyl cellulose is appraised as a homopolymer of anhydroglucose units, featuring hydroxyl groups that provide reactive sites for chemical modification, thereby facilitating the development of ethyl cellulose derivatives and nanostructures [12,13]. Among natural sources, ethyl cellulose can be extracted from wood, cotton, hemp, and agricultural residues. Still, it can also be synthesized by certain bacteria, such as *Komagataeibacter xylinus*, which produce bacterial ethyl cellulose with high purity and unique nanostructures [14]. In nanotechnology, ethyl cellulose is processed into nanoscale forms for diverse applications. Representative examples encompass ethyl cellulose nanofibers for flexible electronic monitoring [15], bacterial nano-ethyl cellulose for skin wound healing [16], and ethyl cellulose nanocrystals for high-performance biodegradable packaging materials [17].

For food packaging, ethyl cellulose has emerged as a promising material considering its biodegradability, non-toxicity, and enhanced barrier properties against oxygen, moisture, and microbial contamination. In addition to these advantages, ethyl cellulose-based NMs are also preferred for the preservation of food products due to their high mechanical strength, transparency, and thermal stability [18]. *Rosmarinus officinalis*, commonly known as rosemary, is a member of the Lamiaceae family. Originating from the Mediterranean region, it is extensively cultivated throughout Europe, Asia, and the Americas. Rosemary is abundant in essential oils, such as 1,8-cineole, α-pinene, camphor, and rosmarinic acid [19]. The scientific evidence about the incorporation of rosemary extracts on NMs for food packaging is limited; for instance, its use has been reported only in gelatin-chitosan films, polyamide-chitosan nanofibers, chitosan films, and nisin-chitosan films for chicken meat [20], strawberry [21], cheese [22], and smoked salmon preservation [23], respectively. Together with this, rosemary extracts have been documented as efficient components in complex mixtures for sausage [24] and sunflower oil storage [25], respectively. The evidence about the incorporation of rosemary-loaded NMs on packaging materials is also

scarce; however, recent studies have demonstrated that, when incorporated in films fabricated with low-density polyethylene and chitosan, they occur in modified systems with promising properties for food packaging as an antioxidant and antimicrobial material [26]. Despite this, its use in the preservation of other products, such as rabbit meat, has not been documented.

Considering the need to develop cost-effective and efficient approaches for rabbit meat packaging, this study aimed to develop ethyl cellulose-NPs loaded with rosemary extracts and incorporate them by spray-drying on HDPE packaging bags. The synthesized formulation was designated as RCL-NPs. The size, surface charge, and polydispersity index (PDI) of RCL-NPs were analyzed by dynamic light scattering (DLS), and release studies were performed to determine the extract release rate in experimental media. Furthermore, RCL-NPs were evaluated for the capability to prevent drained liquid, weight loss, color variability, and pH changes while preserving meat texture and firmness. The retrieved data from this work demonstrated that HDPE packaging bags reinforced with RCL-NPs can preserve the integrity of rabbit meat, suggesting their food packaging potential.

2. Materials and Methods

2.1. TPC, DPPH, and FRAP Activity Analysis of Rosemary Extract

The rosemary extract utilized in this work was commercially obtained from a local supplier in Toluca, Estado de Mexico, Mexico. The TPC of the rosemary extract was analyzed following the Folin–Ciocalteu method and reported as milligrams of gallic acid (GAE) equivalents per gram of the plant extract (mg GAE/g). The calibration curve with GAE was constructed as reported, with minor modifications [27], specifically about the employed wavelength (765 nm). The TPC assay was performed by mixing 200 µL of rosemary extract with 1 mL of Folin–Ciocalteu reagent, and allowed to react for 2 min. After this, 500 µL of a sodium carbonate solution was added, and the sample was vortexed and incubated for 2 h in a dark place at room temperature. The absorbance of the resultant was analyzed in a Genesys 10S UV-Vis spectrophotometer (Thermo Fisher Scientific; Waltham, MA, USA). All experiments were carried out in triplicate.

The antioxidant capacity of rosemary extract was investigated by initially preparing a 95% DPPH (1,1-diphenyl-2-picrylhydrazyl) solution. Similarly, a 95% Trolox solution was also prepared to create the standard curve. Briefly, a dilution of the extract was made by mixing it with 4.79 mL of ethanol until a final concentration of 625 µg/mL. Then, 450 µL of the resultant was mixed with 1050 µL of the stock solution of DPPH. The sample was allowed to react for 30 min in a dark place. The absorbance was measured using a Genesys 10S UV-Vis spectrophotometer (Thermo Fisher Scientific; Waltham, MA, USA) at 517 nm. The antioxidant capacity by the FRAP assay was performed by preparing a 0.3 M acetate buffer solution together with a 20 µM ferrous chloride solution, 40 µM hydrochloric acid solution, and 0.01 M TPTZ (2,4,6-tris(2-pyridyl)-s-triazine), respectively. The solutions were mixed in a 10:1:1 ratio. After this, the rosemary extract was diluted, 20 µL was taken, and mixed with 2 mL of FRAP reagent. The mixture was incubated at 37 °C for 5 min. The absorbance was measured using a Genesys 10S UV-VIS spectrophotometer at 595 nm. The results were reported as µg Trolox equivalents/L. All analyses were performed in triplicate.

2.2. Synthesis, Characterization, Encapsulation Efficiency (EE), and Stability of RCL-NPs

The development of RCL-NPs was performed following the emulsification technique. Briefly, 6.25 µL of rosemary extract was dispersed on a 3% polyvinyl alcohol (PVA) solution together with 0.25 g of ethyl cellulose previously dissolved in 20 mL ethyl acetate. The mixture was maintained under stirring until homogenization. The result was ultrasonicated at 1500 rpm for 10 min utilizing a UP200Ht Ultrasonic Processor (Hielscher Ultrasonics,

Teltow, Germany). The synthesized RCL-NPs were preserved in amber vials under refrigeration at 4 °C. The size and surface charge of the obtained RCL-NPs were recorded utilizing a Zetasizer Nano ZS90 (Malvern Instruments, Worcestershire, UK). The morphology of RCL-NPs was investigated utilizing a Hitachi SU-8230 high-resolution scanning electron microscope (Hitachi High-Technologies Corporation; Tokyo, Japan). The images were acquired utilizing a BSE + BSE(U) detector with a voltage of 2.5 kV and deceleration of 15 kV with an emission current of 5 Å and working distance of 3.7 mm. The EE of RCL-NPs was determined by centrifuging the obtained sample at 15,000 rpm for 60 min at 2 °C in a Z 323 K centrifuge (Hermle, Gosheim, Germany). The supernatant was discarded and utilized to determine the total phenolic content (TPC) utilizing the Folin–Ciocalteu method at 740 nm as previously described [28]. The obtained result was compared with the TPC of the rosemary extract previously dispersed on the PVA solution. Equation (1) was implemented to assess the final EE value. The stability of RCL-NPs was established utilizing a Turbiscan Classic MA 2000 (Formulaction; L'Union, Toulouse, France). For this, samples were diluted and transferred into flat-bottom cylindrical glass cuvettes. The analyses were performed at room temperature, 800 nm, and scanned for 8 min over 24 h. The transmitted light was at 180°, whereas the retro-dispersed light was at 45°.

$$EE\ (\%) = \frac{TPC\ of\ added\ rosemary\ extract - TPC\ of\ the\ supernatant}{TPC\ of\ added\ rosemary\ extract} \times 100 \quad (1)$$

2.3. Incorporation of RCL-NPs into HDPE Packaging Bags, Packaging of Rabbit Meat, and Release Rate Analysis

The synthesized RCL-NPs were incorporated on HDPE packaging bags by spray-drying utilizing an ADIR 684 compressor (ADIR; Istanbul, Turkey), considering a distance of 16 cm and 3 mL of the RCL-NPs solution. This was performed to ensure the heterogenous distribution of the spray-drying. The packaging of rabbit meat was performed by placing 40 g of meat in a 12 cm × 5 cm HDPE and then heat-sealing in a MILTIVAC fume hood (MULTIVAC; Waldkirch, Germany). The packaging material used for the storage of meat samples was Sealed Air™ type, manufactured by Cryovac Mexico (Toluca, Estado de Mexico, Mexico), which supplied the co-extruded food-grade film. The utilized HDPE packaging bags exhibit a thickness of 0.140 mm and a usable width of 13 cm. It has thermal resistance ranging from 75 to 90 °C and sealing temperatures between 130 and 160 °C, as well as a low oxygen transmission rate of 0.33 cm^3/m^2·day and a water vapor transmission rate of 0.26 g/m^2·day under standard conditions (23 °C, 0% RH for oxygen and 38 °C, 90% RH for vapor). This ensures effective protection against oxidation and dehydration of the product. Once the meat was packaged, the samples were stored under refrigeration at 0 °C for 13 d. Figure 1 illustrates the utilized HDPE packaging bags and the refrigerated storage of rabbit meat samples. The release rate of RCL-NPs in HDPE packaging bags was performed following the substitution method. Briefly, a sample of 1 cm^2 of the packaging material was immersed in 10 mL of a 10% ethanol solution and subjected to constant agitation. Samples were collected every 15 min during the initial 2 h. Subsequently, the sampling interval was extended to 30 min over the following 8 h. Finally, samples were taken until the completion of a 24 h analysis period. The absorbance of all samples was measured using a Genesys 10S UV-Vis spectrophotometer (Thermo Fisher Scientific; Waltham, MA, USA) at 207 nm. Rabbit meat samples conserved in HDPE packaging bags without RCL-NPs were appraised as a control. All experiments were performed in triplicate.

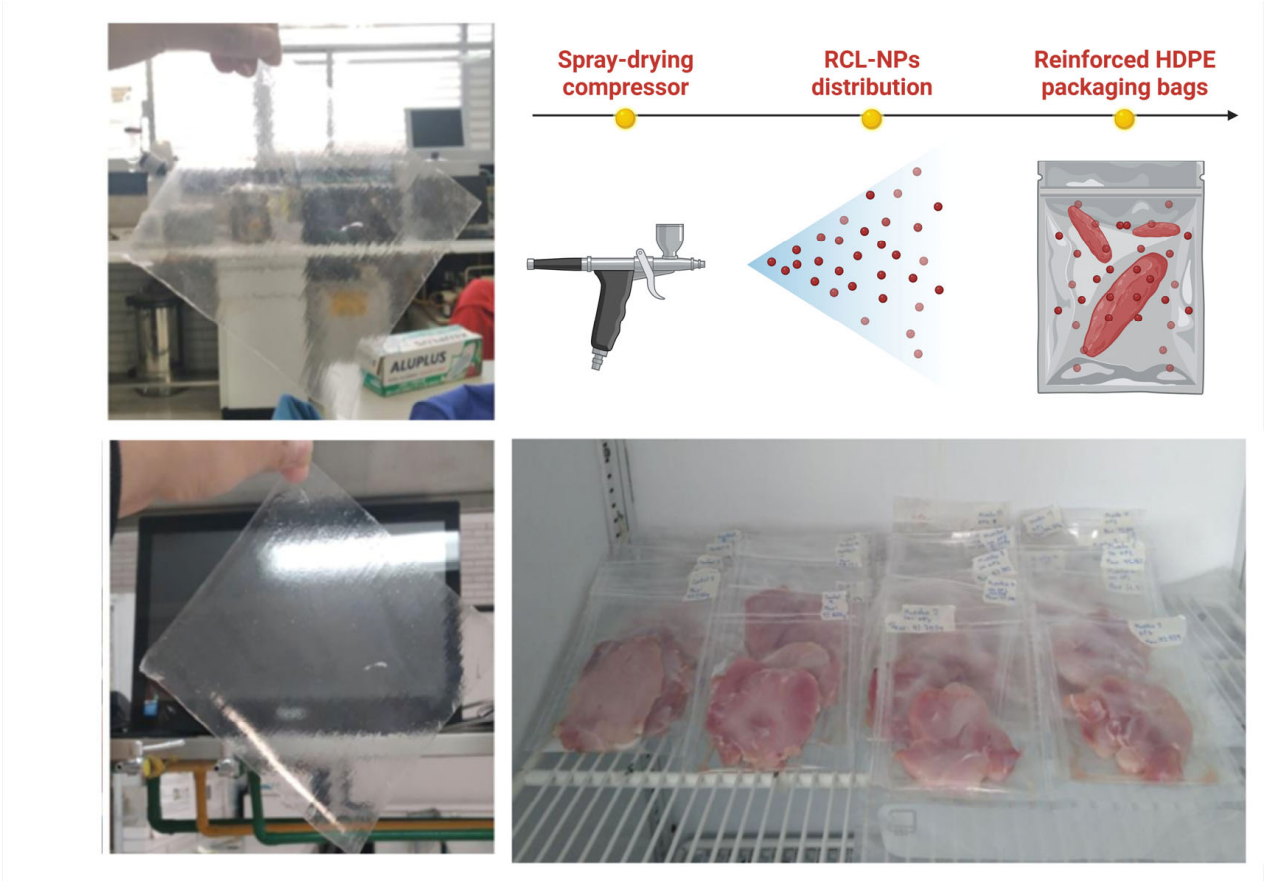


Figure 1. Representation of the utilized HDPE packaging bags, spray-drying of RCL-NPs, and storage conditions of rabbit meat samples utilized in this study.

2.4. Drained Liquid and Weight Loss Analysis

The drained liquid was measured with a graduated syringe, which was carefully inserted into the bottom of the utilized HDPE packaging bags. The weight loss analysis of samples was assessed considering the difference between the initial weight of the packaged rabbit meat (40 g) and the weight after 1, 3, 6, 8, 10, and 13 days of storage. Rabbit meat samples conserved in HDPE packaging bags without RCL-NPs were appraised as a control. All experiments were performed in triplicate.

2.5. Color and pH Analysis

The color variabilities among rabbit meat samples conserved in HDPE packaging bags were investigated using a Minolta CM-600d spectrophotometer (Konica Minolta Inc., Tokyo, Japan). The determined coordinates encompass *L, *a, and *b values. The evaluation of the pH of samples was performed with a Hanna HI99163 potentiometer (Hanna Instruments; Woonsocket, RI, USA). The analysis of samples was executed after 1, 3, 6, 8, 10, and 13 days of storage, respectively. Rabbit meat samples conserved in HDPE packaging bags without RCL-NPs were appraised as a control. All experiments were conducted in triplicate.

2.6. Texture and Hardness Analysis

The texture and hardness of samples were recorded using a Texture Analyzer CT3 Brookfield (Brookfield Engineering Laboratories; Middleboro, MA, USA). For the former, Rabbit leg samples were cut into 1.5 cm × 1.5 cm × 0.5 cm pieces and placed parallel to the cylinder to ensure uniform compression along the axis perpendicular to the surface. For the texture analysis, two consecutive compression cycles (cycle 1 and cycle 2) were conducted without any waiting time between them. Compression was applied to 50% of the sample

thickness, using an activation load of 0.07 N. The pre-test speed was set at 3 mm/s, while the post-test speed was reduced to 1 mm/s. For the hardness analysis, the dimensions of the rabbit leg samples were 2 cm in length, 2 cm in width, and 0.5 cm in thickness. These samples were positioned parallel to the edge of the probe to ensure a uniform cross-section during testing. The test was conducted at a speed of 5 mm/s, with a trigger load set at 0.10 N and a target distance of 23 mm. All experiments were performed in triplicate.

2.7. Statistical Analysis

A one-way analysis of variance (ANOVA) followed by Tukey's mean separation test was executed to assess significant statistical differences in GraphPrad.

3. Results

3.1. TPC and Antioxidant Activity of Rosemary Extract

According to the calibration curve of GAE and the retrieved regression equation presented in Figure S1 ($y = 0.3327x + 0.0044$; $R^2 = 0.994$), the TPC of rosemary extract was 566.13 ± 1.72 mg GAE/L. As illustrated in Figure S2, the calculated scavenging activity of rosemary extract was 27.86 ± 0.32 mM Trolox/L. The determined FRAP activity of the same sample was 0.31 mM Trolox/L. The DPPH result was in accordance with the regression equation obtained from the calibration curve with Trolox: $y = -7.5475x + 1.5746$; $R^2 = 0.9776$.

3.2. Synthesis and Characterization of RCL-NPs

As illustrated in Figure 2A, the average size of RCL-NPs was 117.30 ± 0.55 nm. The surface charge of RCL-NPs was −24.59 ± 4.76 mV, which is depicted in Figure 2B. The PDI of the synthesized RCL-NPs was 0.127 ± 0.01. As noted in Figure 2C, the stability analysis of RCL-NPs did not present significant peaks associated with flocculation or sedimentation, suggesting their stability and homogeneity. According to Figure 2D, the developed RCL-NPs are spherical with a smooth surface.

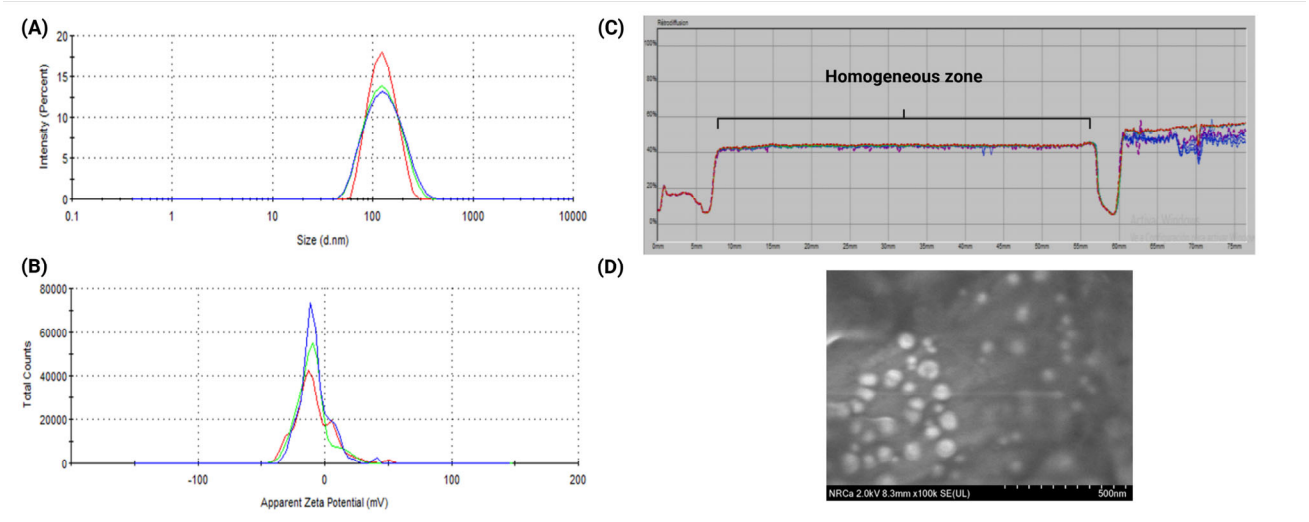


Figure 2. DLS analysis of the (**A**) size distribution, (**B**) surface charge, (**C**) light backscattering analysis, and (**D**) SEM evaluation of RCL-NPs. The blue, green, and red lines represent independent experiments.

3.3. EE and Release Profile of RCL-NPs

Considering Equation (1), the calculated EE of RCL-NPs was 99.97%. As demonstrated in Figure S3, the release of rosemary extract from CL-NPs occurred over a 10 h period, ranging from 0.07 ± 0.01 to 0.83 ± 0.12 µL/mL. Similarly, the release of rosemary extract

from CL-NPs was 0.86 ± 0.12, 0.89 ± 0.14, and 0.98 ± 0.15 µL/mL. Figure S3 also presents the release profile of rosemary extract from RCL-NPs modeled by the zero- and first-order model, as well as the Higuchi model, the Korsmeyer-Peppas model, and the Weibull model. The fitted parameters and correlation coefficients from each model are listed in Table 1.

Table 1. Kinetic models, fitted parameters, and correlation coefficients for the release of rosemary extract from RCL-NPs.

Model	Equation	Kinetic Constants	R^2
Zero-order	$M_t = k_0 t + C_0$	K_0 = 0.0629	0.871
First-order	$Ln(M_\infty - M_t) = LnM_\infty - k_1 t$	k_1 = 0.139	0.789
Higuchi	$M_t = k_H t^{\frac{1}{2}} + C$	k_H = 0.216	0.9469
Korsmeyer-Peppas	$\frac{M_t}{M_\infty} = kt^n$	k = 0.636; n = 0.459	0.951
Weibull	$\frac{M_t}{M_\infty} = 1 - exp\left[-(t/\propto)^\beta\right]$	α = 0.3566; β = 0.491	0.968

3.4. Drained Liquid and Weight Loss Analysis

As noted in Figure 3A, the drained liquid with samples appraised as control was 0.36 ± 0.15 and 0.53 ± 0.11% after 3 and 6 days, whereas at 8 and 10 days, the drained liquid was 0.60 ± 0.10 and 0.76 ± 0.30%, respectively. After 13 days, the drained liquid was 0.93 ± 0.49% among the samples considered as a control.

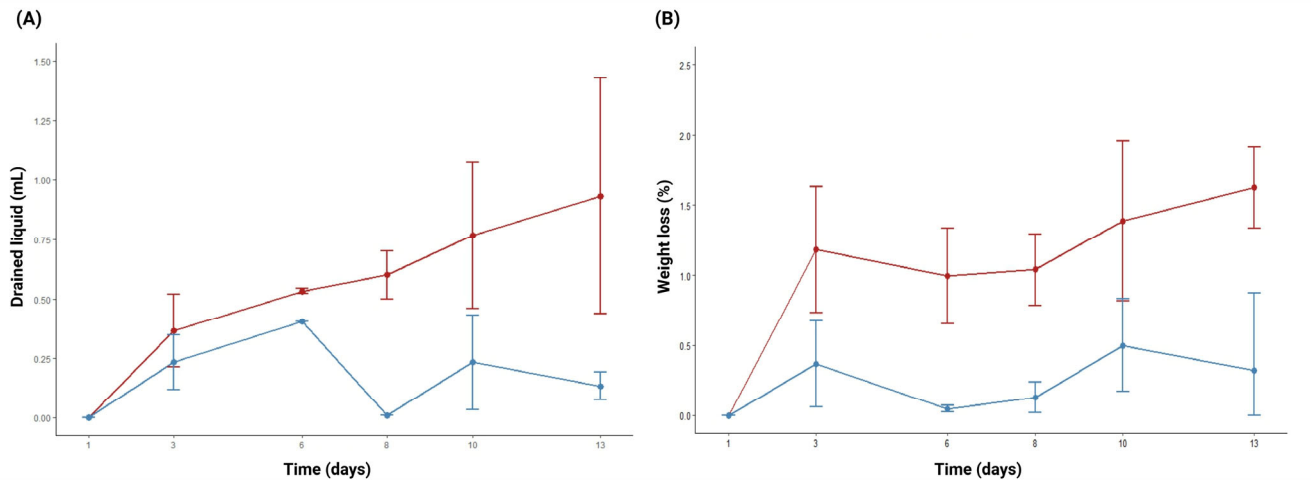


Figure 3. (**A**) Drained liquid and (**B**) weight loss of rabbit meat samples. The red line is associated with control samples, whereas the blue line is correlated with samples conserved in HDPE packaging bags reinforced with RCL-NPs. Shown is the mean ± S.D. of three independent experiments.

In Figure 3A, it can also be observed that the drained liquid of the samples after preservation with HDPE packaging bags reinforced with RCL-NPs was 0.23 ± 0.11%, 0.40 ± 0.68%, and 0.01 ± 0.05% at 3, 6, and 8 days, respectively. The drained liquid from rabbit meat samples preserved with RCL-NPs showed statistically significant differences at days 6 ($p < 0.001$) and 8 ($p < 0.01$) compared to the control samples. The recorded drained liquid at 10 and 13 days among samples with HDPE packaging bags reinforced with RCL-NPs was 0.23 ± 0.23 and 0.13 ± 0.05%, respectively. According to Figure 3B, the weight loss after 3, 6, and 8 days of preservation with RCL-NPs was 0.36 ± 0.30, 0.04 ± 1.38, and 0.12 ± 0.10%, respectively. After 10 and 13 days of preservation with RCL-NPs, the weight loss was 0.50 ± 0.50 and 0.32 ± 0.55%, respectively. Contrary to this, the weight loss of the samples used as controls at 3 and 6 days was 1.18 ± 0.44% and 0.99 ± 0.33%,

whereas the samples at 8, 10, and 13 days after preservation presented a weight loss of 1.03 ± 0.25%. 1.38 ± 0.56, and 1.62 ± 1.00% weight loss, respectively (see Figure 3B). According to statistical analysis, the weight loss of rabbit meat preserved with RCL-NPs was statistically different at days 8, 10, and 13 ($p < 0.05$), respectively.

3.5. Color and pH Analysis

As demonstrated in Figure 4A, the *L** values of rabbit meat samples conserved in HDPE packaging bags reinforced with RCL-NPs after 1, 3, and 6 days were 56.20 ± 2.40, 61.20 ± 5.20, and 56.60 ± 2.40, respectively. After 8, 10, and 13 days, the *L** values for the same samples were 60.50 ± 2.5, 59.10 ± 2.30, and 66.10 ± 2.50, respectively.

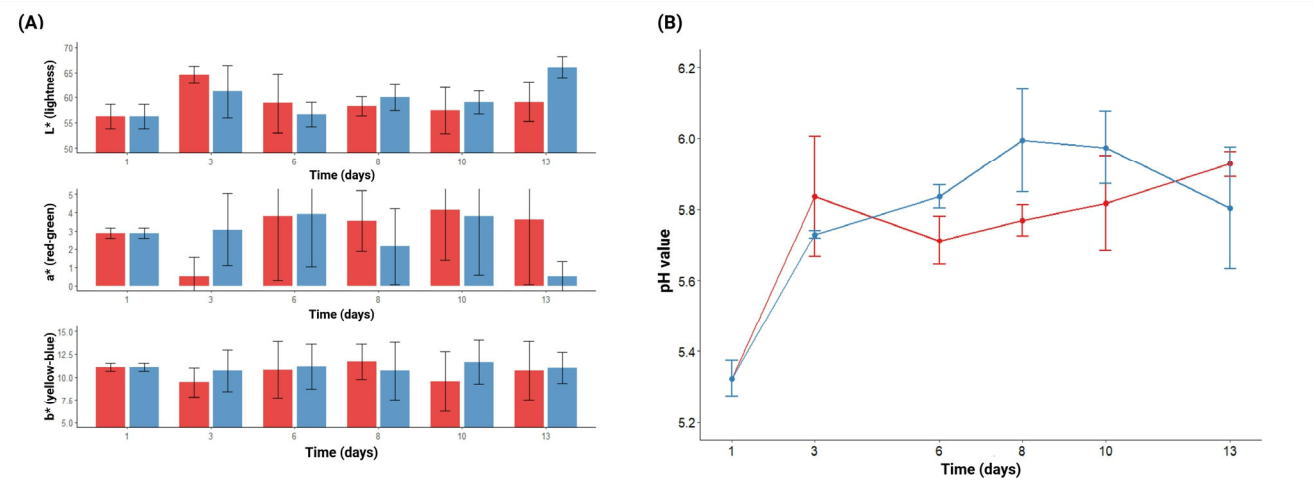


Figure 4. (**A**) Color and (**B**) pH analysis of rabbit meat samples. The red bar or line is associated with control samples, whereas the blue bar or line is correlated with samples conserved in HDPE packaging bags reinforced with RCL-NPs. Shown is the mean ± S.D. of three independent experiments.

Similarly to these findings, it was noted that the preservation of rabbit meat control samples exhibited *L** values of 56.18 ± 2.40 and 64.56 ± 1.70 after 1 and 3 days during storage, respectively. Comparably, it was determined that the *L** values after 6, 8, 10, and 13 days were 58.85 ± 5.80, 58.24 ± 1.90, 57.39 ± 4.50, and 59.10 ± 3.80, respectively (see Figure 4A). As represented in Figure 4, the a* values of rabbit meat conserved in HDPE packaging bags reinforced with RCL-NPs were 2.89 ± 0.27, 3.08 ± 1.96, and 3.92 ± 2.89 after 1, 3, and 6 days, respectively. At 10 and 13 days, the *a**values conserved with the same treatment were 3.81 ± 3.22 and 0.50 ± 0.82, respectively. When evaluated in control samples, the a* values at 1, 3, and 6 days were 2.89 ± 0.27, 0.53 ± 1.50, and 3.82 ± 3.51. On 8 and 10 days, the *a** values were 3.54 ± 1.60 and 4.15 ± 2.70, whereas on 13 days, the *a** value was 3.62 ± 3.50 (see Figure 4). The *b** values of rabbit meat samples conserved in HDPE packaging bags reinforced with RCL-NPs were 11.08 ± 0.46 and 10.67 ± 2.28 at 1 and 3 days, whereas at 6 and 8 days, the *b** values were 11.50 ± 2.47 and 10.67 ± 3.15, respectively. The *b** values at 10 and 13 days the *b** values were 11.62 ± 2.39 and 11.00 ± 1.69 after c preservation with HDPE packaging bags reinforced with RCL-NPs. For control samples, the *b** values ranged from 11.08 to 10.68 after the evaluated days during storage. No statistical differences were found between color changes from rabbit meat samples preserved with RCL-NPs and those used as controls. As illustrated in Figure 4B, the pH of samples conserved in HDPE packaging bags reinforced with RCL-NPs were 5.73 ± 0.01, 5.83 ± 0.03, and 5.99 ± 0.14 after 3, 6, and 8 days during storage, respectively. After 10 and 13 days, the pH values of the same samples were 5.97 ± 0.10 and 5.80 ± 0.17, respectively. The pH of control samples was 5.83 ± 0.16 and 5.71 ± 0.06 after 3 and 6 days of storage, whereas after 8 and 10 days, the pH was 5.77 ± 0.04 and 5.81 ± 0.13, respectively. On day 13,

the pH of control samples was 5.92 ± 5.80. No statistical differences were found between the pH of rabbit meat samples preserved with RCL-NPs and those used as controls.

3.6. Texture and Hardness Analysis

The texture of control samples was 7.62 ± 4.11, 2.03 ± 1.31, and 1.14 ± 0.56 N after 3, 6, and 8 days of preservation after cycle 1, respectively. After 10 days during the same cycle, the texture of the control sample was 0.87 ± 0.50 N. During cycle 2, the texture of control samples was 6.33 ± 4.21 and 1.93 ± 0.97 after 3 and 6 days, whereas at 8 and 10 days after preservation, the determined texture was 1.20 ± 0.59 and 0.85 ± 0.54 N, respectively. Figure 5A also illustrates that the texture of rabbit meat after preservation with HDPE packaging bags reinforced with RCL-NPs was 3.19 ± 1.46 and 1.07 ± 0.48 N, respectively. After 8 and 10 days of preservation with the same samples, the texture was 0.78 ± 0.34 and 0.70 ± 0.52 N, respectively. This was recorded after cycle 1, whereas after cycle 2, the same figure represents that the texture of rabbit meat was 2.87 ± 1.27, 0.97 ± 1.27, and 0.70 ± 0.31 N after 3, 6, and 8 days, respectively. After 10 days in preservation, the texture was 0.61 ± 0.46 (see Figure 5B). Regarding texture variations, no statistical differences were found between rabbit meat samples preserved with RCL-NPs and those used as controls.

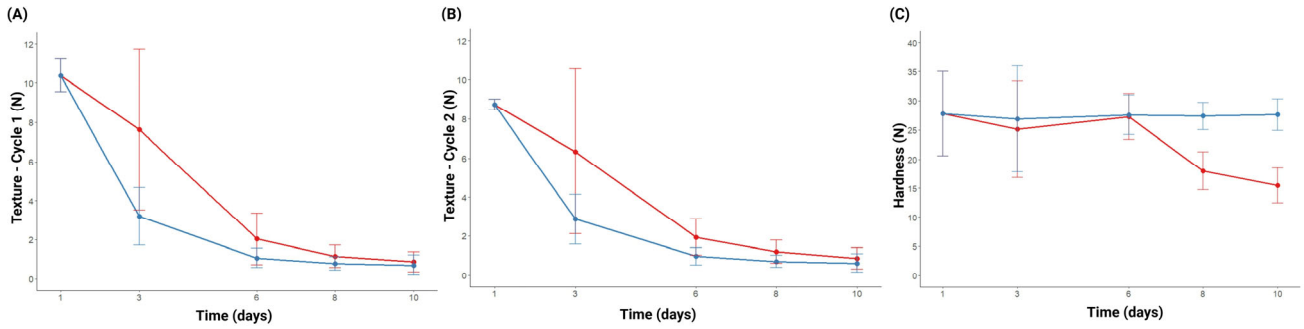


Figure 5. Texture analysis after (**A**) cycle 1 and (**B**) cycle 2, and (**C**) texture evaluation of rabbit meat samples. The red line represents control samples, whereas the blue line is correlated with samples conserved in HDPE packaging bags reinforced with RCL-NPs. Shown is the mean ± S.D. of three independent experiments.

As represented in Figure 5C, the hardness of samples utilized as controls was 25.11 ± 8.26, 27.29 ± 3.88, and 17.99 ± 3.23 N, respectively. After 10 days of preservation, the hardness of samples was 15.46 ± 3.05 N. Similarly, samples conserved in HDPE packaging bags reinforced with RCL-NPs exhibit a texture of 26.88 ± 9.02 and 27.57 ± 3.39 N after 3 and 6 days of preservation. At 8 and 10 days, the recorded texture was 27.38 ± 2.31 and 27.60 ± 2.69 N, respectively. The statistical analysis did not reveal any statistically significant differences between rabbit meat samples preserved with RCL-NPs and those used as controls.

4. Discussion

Food packaging is necessary for preserving the quality and extending the shelf life of rabbit meat. Current approaches to rabbit meat preservation face several limitations; for example, traditional packaging materials like polyethylene and polypropylene provide inadequate barriers against oxygen and moisture, leading to oxidation and microbial growth [29]. Even though synthetic preservatives enhance the shelf life of rabbit meat-based products, they also pose potential health risks by causing endocrine disruption or allergic reactions [30]. Vacuum or modified atmosphere packaging has also been explored for rabbit-meat preservation; however, it can cause discoloration, texture changes, and require specialized equipment and careful gas composition control [31].

As an alternative to current approaches for rabbit-beat preservation, this work reported the use of RCL-NPs to reinforce HDPE packaging bags for the preservation of rabbit meat. Regarding the development of RCL-NPs, it was determined by DLS that they exhibit an average hydrodynamic diameter of 117.30 nm with a PDI of 0.127 and surface charge of −24.50 nm. The hydrodynamic size of NPs alludes to the effective diameter of a particle in solution, including any layers of solvent or molecules adsorbed to its surface. The hydrodynamic size of NPs is significant to determine since it influences the particles' behavior in the packaging material and their interaction with food components. Considering current classifications of the nanoscale, NMs with high hydrodynamic size (>1000 nm) tend to exhibit aberrations in their dispersion and stability when integrated on packaging materials. Contrary, NMs with a smaller hydrodynamic size (<300 nm) pose enhanced incorporation capacity on packaging materials and enhanced barrier properties. The PDI of polymer-based NMs indicates their distribution in organic or inorganic samples, where low PDI (<0.3) values suggest their uniform distribution, a feature desirable for consistent performance in food packaging, predictable behavior, and improved barrier effectiveness and antimicrobial activity. Together with these features, surface charge, also known as ζ-potential, determines the stability and interaction between NMs with food components. Considering this, a higher surface charge (+30 or −30 mV) indicates high electrostatic repulsion between particles, leading to better colloidal stability. In food packaging, surface charge can influence NMs' ability to interact with food molecules or packaging materials, affecting their functionality and potential migration.

Light backscattering is a highly sensitive, non-destructive tool for assessing the physicochemical stability of colloidal systems. Here, RCL-NPs showed no typical instability phenomena such as creaming, sedimentation, coalescence, or flocculation, indicating a homogeneous and stable colloidal structure. The narrow size distribution implied uniform distribution and adequate surface stabilization, given the recorded zeta potential associated with the surfactant used, which stabilizes the pH, ionic strength of the medium, and organic material present. These factors modify the electrostatic interactions between particles, particularly through alterations in the zeta potential and thickness of the electrical double layer. The stability observed in the samples suggests that the system conditions were controlled.

Encapsulation is a fundamental technique in food packaging that involves the entrapment of active ingredients within a protective layer [32]. In the food industry, encapsulation has been leveraged to preserve and enhance the biological performance of organic substances with antimicrobial, antioxidant, and flavoring capabilities [33]. Additionally, it has been utilized to fulfill the primary functions of traditional packaging materials by protecting the physical, chemical, and biological integrity of sensitive substances from exposure to light, air, and moisture [33], as well as preventing undesirable reactions with food [34]. Here, it was recorded that the EE of the developed ethyl cellulose-NPs was 99.97%, which can be attributed to its negative surface charge (−24.59 mV). This surface charge may enhance the interactions between the functional groups on the surface of RCL-NPs and the compounds contained in the encapsulated extract, leading to improved encapsulation. Similarly, the use of the ultrasonic probe can be considered as another factor that contributed to the high EE of the developed NPs, since it has been reported that the generated high-frequency sound waves can create microbubbles in the medium. When collapsed, bubbles can disrupt ethyl cellulose fibers, resulting in NPs with an enhanced surface area for encapsulation. Together with this, the sonication time has been documented to increase the dispersion and loading capacity of polymer-based NPs.

The release efficiency of entrapped substances on NMs can occur through various mechanisms, such as diffusion, degradation, and stimuli-responsive release [35]. There

are numerous factors influencing the release profiles of entrapped substances, for example, material selection and the presence or absence of surface modification. Given the polysaccharide-based nature of ethyl cellulose, release mechanisms often documented are diffusion, swelling, and degradation processes [36]. In contrast to diffusion and degradation, selling results when ethyl cellulose-based NMs encounter aqueous environments, where the absorption of water or phosphate-buffered solutions can cause the formation of larger pores within the nanostructure [37]. Even though this mechanism is often observed when entrapping substances on ethyl cellulose-based NMs, it can vary between reports, considering the degree of substitution and cross-linking density of the employed precursors. In food packaging development, investigating the release efficiency of NMs is crucial for optimizing formulations, predicting product shelf life, and ensuring the efficacy of ingredients during storage. Here, it was noted that the release kinetics of RCL-NPs displayed a typical biphasic behavior. Initially, a rapid release was observed during the first 4 to 6 h, followed by a significant decrease in the release rate. This pattern is characteristic of diffusion-dominated release systems. In this context, the extract located on the surface of the nanoparticles is released quickly into the surrounding medium, while the extract trapped within the polymeric matrix is released at a much slower rate. This slower release is attributed to the resistance provided by the ethylcellulose used as the wall polymer in this study. Notably, after 10 h, the release stabilizes, as the extract becomes strongly retained within the encapsulating polymer matrix. The retrieved results were evaluated by a zero- and first-order model, together with the Higuchi, Korsmeyer-Peppas, and Weibull models, respectively.

Upon implementation, it was observed that neither zero-order nor first-order kinetics accurately described the observed release rate. In contrast, the Higuchi model provided a better fit, suggesting that the release process is governed by Fickian diffusion, a characteristic of polymeric matrices such as ethylcellulose. The Korsmeyer-Peppas model, applied to the first 60% of the accumulated release, also demonstrated a strong fit with an n value of 0.478, confirming Fickian diffusion without significant relaxation of the matrix. Additionally, the Weibull model exhibited an improved fit, indicating a sigmoidal, diffusion-controlled release characterized by a rapid initial phase followed by a gradual deceleration. Considering the performed kinetic analyses, it can be noted that the release of rosemary extract from RCL-NPs primarily occurs through diffusion-controlled mechanisms, particularly during the initial stages. During this process, the ethylcellulose matrix can serve as a release barrier, effectively modulating the transfer of rosemary extract from the packaging to the product, thereby enhancing its preservative action. The fits obtained from the Korsmeyer-Peppas and Weibull models accurately describe this behavior and enable predictions of the release profile under storage conditions for the preservation of rabbit meat. Thus, these parameters are crucial for designing active packaging systems that facilitate controlled release in food applications [38,39].

Determining the TPC of extracts intended for food packaging is crucial for assessing their antioxidant capacity, overall efficacy, and provides valuable insights on the extract's potential to inhibit oxidative processes, microbial growth, and extend the shelf life of products [40]. Antioxidant activity refers to the capacity of a substance to inhibit oxidation processes. In the context of food packaging, the antioxidant activity of NMs or encapsulated substances is crucial for neutralizing free radicals and other reactive oxygen species that can cause oxidative damage to food components or lead to rancidity, discoloration, and nutrient degradation in food products [41]. The TPC of rosemary extract-based preparations has been widely documented, especially for extracts and powders obtained from natural sources. However, they tend to vary due to the utilized raw material, environmental conditions, seasonality, and selected extraction method. For these reasons, commercially

available extracts are preferred as they are standardized to ensure their composition, purity, and documented efficacy.

Drained liquid is the term designated to the liquid that separates from solid food components during storage, often accumulating at the bottom of the package. This phenomenon is especially relevant for meat products, where the exudation of moisture can significantly impact quality and consumer acceptance [42]. The amount of drained liquid is an indicator of moisture retention capacity and overall product stability. Excessive liquid loss can lead to textural changes, nutrient leaching, and increased microbial growth risk [43]. In the development of NMs intended for food packaging, the scientific evidence quantifying drained liquid is limited, even though it can provide valuable insights into their capacity to enhance product quality, extend shelf life, and sensory attributes. Meat weight loss is a critical parameter in food packaging research, defined as the reduction in mass of meat products during storage or processing. This phenomenon is primarily caused by moisture loss, protein denaturation, and fat oxidation [44]. Factors influencing meat weight loss include temperature, relative humidity, packaging permeability, and microbial activity. The consideration of meat weight loss is crucial for evaluating since it directly influences the economic value of the product, together with its texture, juiciness, and sensory quality [45]. The retrieved data from the drained liquid and meat weight loss is challenging to compare since there are no reports demonstrating the preservation performance of ethyl cellulose-based NMs, specifically in rabbit meat.

Color is essential in quality assessment of rabbit meat, where the L^*, a^*, and b^* color coordinates provide an objective measure of meat lightness, redness, and yellowness, respectively. Monitoring variabilities in L^*, a^*, and b^* values over time can reveal oxidation processes, microbial growth, or other quality deterioration factors [46]. When developing packaging materials, determining these color coordinates is necessary for assessing the effectiveness of the packaging in maintaining the meat's visual appeal [47]. Packaging that preserves the initial color values of fresh rabbit meat for longer periods demonstrates superior performance and efficacy during food packaging. The pH of meat-based products is directly correlated with protein stability, water-holding capacity, texture, juiciness, and overall meat quality during storage. Additionally, as meat pH increases post-mortem, it becomes more susceptible to bacterial proliferation, leading to spoilage and reduced shelf life [48]. Furthermore, pH levels correlate with color stability and lipid oxidation, key factors in consumer acceptance, safety, and quality throughout the product's shelf life [49]. Texture and hardness are critical quality parameters in evaluating rabbit meat and designing appropriate packaging materials. Texture refers to the sensory perception of the meat's structure and organization, encompassing attributes like tenderness, juiciness, and chewiness [50]. Hardness, a component of texture, specifically relates to the meat's resistance to deformation when force is applied. These characteristics are essential for consumer acceptance and can indicate the meat's freshness and marketability [51]. Effective packaging should maintain the meat's original texture and firmness by minimizing moisture loss, preventing protein denaturation, and inhibiting microbial growth.

5. Conclusions

In this study, RCL-NPs were synthesized via the emulsification route and incorporated into HDPE packaging bags utilizing a spray-drying technique. When analyzed by DLS, it was unveiled that RCL-NPs were 117.30 nm in size, with a negative surface charge of −24.59 mV, and a low PDI of 0.12, suggesting their stability and low tendency to agglomerate. The employed synthesis method yielded RCL-NPs with an efficiency of 99.97%. The TPC of the rosemary extract was 566.13 ± 1.72 mg GAE/L, while its antioxidant activity, measured using the DPPH and FRAP assays, was 27.86 ± 0.32 mM

Trolox/L and 0.31 mM Trolox/L, respectively. Rabbit meat stored in HDPE bags reinforced with RCL-NPs showed no drained liquid or weight loss, while maintaining *L^* (60 ± 2.5–66.10 ± 2.0) and *b^* (10.67 ± 2.28–11.62 ± 2.39), pH (5.22 ± 0.05–5.80 ± 0.03), and texture (10.37 ± 0.82–0.70 ± 0.50). The hardness of the rabbit meat samples conserved in HDPE packaging bags reinforced with RCL-NPs ranged from 27.79 ± 7.23 to 27.60 ± 3.05 N over 0–13 days. Even though the collected data confirm the effectiveness of RCL in maintaining the quality of rabbit meat, further spectroscopy and microscopy are necessary to demonstrate the influence of physical, chemical, and mechanical features on the evaluated product. In addition, further assays are required to assess the capacity of the developed approach in avoiding microbial growth.

Supplementary Materials: The following supporting information can be downloaded at: https://www.mdpi.com/article/10.3390/polysaccharides6030076/s1. Figure S1, Calibration curve of GAE for determining the TPC of rosemary extract; Figure S2, DPPH curve for determining the antioxidant activity of rosemary extract. Figure S3. Release profiles of RCL-NPs analyzed by different kinetic models: the zero-order and first-order models, the Higuchi model, the Korsmeyer-Peppas model, and the Weibull model.

Author Contributions: Conceptualization, M.d.l.L.Z.-Z., J.E.A.-T., R.G.C.-M. and M.R.-E.; validation, M.d.l.L.Z.-Z., J.E.A.-T., R.G.C.-M., M.R.-E. and J.L.M.-M.; investigation, B.S.-C., M.d.l.L.Z.-Z., J.E.A.-T., R.G.C.-M. and M.R.-E.; writing—original draft preparation, B.S.-C. and J.L.M.-M.; writing—review and editing, M.d.l.L.Z.-Z., J.E.A.-T., R.G.C.-M., M.R.-E. and J.L.M.-M.; visualization, B.S.-C. and J.L.M.-M.; supervision, M.d.l.L.Z.-Z., J.E.A.-T., R.G.C.-M. and M.R.-E.; funding acquisition; M.d.l.L.Z.-Z., J.E.A.-T., R.G.C.-M., M.R.-E. and J.L.M.-M.; project administration, M.d.l.L.Z.-Z. All authors have read and agreed to the published version of the manuscript.

Funding: This research received no external funding.

Institutional Review Board Statement: Not applicable.

Data Availability Statement: Data generated from this work are contained within the article. Further inquiries can be directed to the corresponding author.

Conflicts of Interest: The authors declare no conflicts of interest.

References

1. Siddiqui, S.A.; Gerini, F.; Ikram, A.; Saeed, F.; Feng, X.; Chen, Y. Rabbit Meat—Production, Consumption and Consumers' Attitudes and Behavior. *Sustainability* **2023**, *15*, 2008. [CrossRef]
2. Kim, J.M.; Park, H.J.; Bae, H. Study on the Impact of Reducing Aluminium Foil Thickness on the Barrier Properties of Retort Pouches During Shelf Life: Simulated Physical Stress Considering Distribution Environment. *Packag. Technol. Sci.* **2025**, *38*, 333–341. [CrossRef]
3. Ferri, M.; Lenzi, L.; Degli Esposti, M.; Martellosio, L.; Benítez, J.J.; Hierrezuelo, J.; Grifé-Ruiz, M.; Romero, D.; Guzmán-Puyol, S.; Heredia-Guerrero, J.A.; et al. Triphenyl Acetic Glyceroate as a Sustainable Multifunctional Additive for Developing Transparent, Biodegradable, and Flexible Polylactide Green Alternative to Polyethylene-Based Films for Food Packaging. *Chem. Eng. J.* **2025**, *508*, 160887. [CrossRef]
4. Xavier, J.R.; Vinodhini, S.P.; Priyadharshini, A. Multifunctional Epoxy-Based Nanocomposite Coating for Tinplate: Enhancing Food Packaging with Superior Mechanical, Anticorrosion, and Antimicrobial Properties. *Int. J. Biol. Macromol.* **2025**, *309*, 142671. [CrossRef]
5. Contreras-López, G.; Morales-Rodríguez, S.; Alarcon-Rojo, A.D.; Carrillo-Lopez, L.M. Effect of Packaging Thickness and Muscle Type on Ultrasound-Assisted Beef Quality. *Ultrason. Sonochemistry* **2024**, *103*, 106777. [CrossRef]
6. Zain Ul Abidin, M.; Ikram, M.; Moeen, S.; Nazir, G.; Kanoun, M.B.; Goumri-Said, S. A Comprehensive Review on the Synthesis of Ferrite Nanomaterials via Bottom-up and Top-down Approaches Advantages, Disadvantages, Characterizations and Computational Insights. *Coord. Chem. Rev.* **2024**, *520*, 216158. [CrossRef]
7. Chang, R.-Y.; Geng, W.-H.; Jing, L.-C.; Feng, J.-Y.; Wang, Y.-X.; Qian, P.-F.; Bao, Z.-L.; Wang, W.; Zhang, D.; Geng, H.-Z. Construction and Application of Antimicrobial Ultrafiltration Membranes Based on Electro-Stimulated Hollow Mesoporous Carbon Spheres and Carbon Nanotubes. *J. Environ. Chem. Eng.* **2025**, *13*, 115773. [CrossRef]

8. Bal, K.; Gök, M.K.; Demir, K.; Özgümüş, S. Building Effective Nanocarriers Based on β-Ionone Loaded 2nd and 3rd Generation L-Arginine Dendrimers: In Vitro Evaluation of Cytotoxicity and Antiproliferative Activity for HeLa Cells. *Mater. Today Chem.* **2025**, *44*, 102545. [CrossRef]
9. Zare, I.; Zahed Nasab, S.; Rahi, A.; Ghaee, A.; Koohkhezri, M.; Ramezani Farani, M.; Madadi Gholipour, H.; Atabaki, A.H.; Hamblin, M.R.; Mostafavi, E.; et al. Antimicrobial Carbon Materials-Based Quantum Dots: From Synthesis Strategies to Antibacterial Properties for Diagnostic and Therapeutic Applications in Wound Healing. *Coord. Chem. Rev.* **2025**, *522*, 216211. [CrossRef]
10. Surya, S.; Soman, A.; Krishnan, A.; Suresh, M.P.; Neenu, K.V.; Ajithkumar, T.G.; Parameswaranpillai, J.; Sabura Begum, P.M.; Midhun Dominic, C.D. Sustainable Cellulose Nanofiber Extraction from *Borassus flabellifer*: A Comprehensive Study and Analytical Insights. *Biomass Conv. Bioref.* **2025**. [CrossRef]
11. Zou, Y.; Liao, Z.; Zhang, R.; Song, S.; Yang, Y.; Xie, D.; Liu, X.; Wei, L.; Liu, Y.; Song, Y. Cellulose Nanofibers/Liquid Metal Hydrogels with High Tensile Strength, Environmental Adaptability and Electromagnetic Shielding for Temperature Monitoring and Strain Sensors. *Carbohydr. Polym.* **2025**, *348*, 122788. [CrossRef]
12. Nandi, S.; Nayak, P.P.; Guha, P. Valorization of Betel Leaf Industry Waste: Extraction of Cellulose Nanocrystals and Their Compatibility with Starch-Based Composite Films. *Biomass Bioenergy* **2025**, *194*, 107678. [CrossRef]
13. Baron, R.I.; Biliuta, G.; Bejan, D.; Darie-Nita, R.-N.; Coseri, S.; Dinu, M.V. Advancing the Design of Conductive Composite Cryogels Based on Hydroxypropyl Cellulose Derivatives for Improving the Compressibility and Anti-Freezing Properties. *Int. J. Biol. Macromol.* **2025**, *296*, 139764. [CrossRef] [PubMed]
14. Huang, L.; Zhou, Y.; Feng, Y.; Jia, S.; Wang, S.; Zhong, C. Tailoring Bacterial Cellulose through the CRISPR/Cas9-Mediated Gene Editing Tool in *Komagataeibacter xylinus*. *ACS Synth. Biol.* **2025**, *14*, 1161–1172. [CrossRef] [PubMed]
15. Zhu, Z.; Zhao, Y.; Zhang, Y.; Zhang, S.; Li, W.; Ye, G.; Ma, X.; Zhang, X.; Bi, H. Self-Healing, Highly Stretchable, and 3D Printable Thiol-Functionalized Cellulose Nanofibers/Waterborne Polyurethane Composites for Flexible Electronic Monitoring. *Chem. Eng. J.* **2025**, *506*, 159835. [CrossRef]
16. Brugnoli, M.; Carvalho, J.P.F.; Arena, M.P.; Oliveira, H.; Vilela, C.; Freire, C.S.R.; Gullo, M. Co-Cultivation of *Komagataeibacter Sp.* and *Lacticaseibacillus Sp.* Strains to Produce Bacterial Nanocellulose-Hyaluronic Acid Nanocomposite Membranes for Skin Wound Healing Applications. *Int. J. Biol. Macromol.* **2025**, *299*, 140208. [CrossRef]
17. He, R.; Gai, L.; Zhu, Z.; Gu, H.; Sun, P. Industrial By-Products of Tiger Nut Starch as a Source of Cellulose Nanocrystals for Biodegradable Packaging Materials. *Int. J. Biol. Macromol.* **2025**, *306*, 141422. [CrossRef]
18. Wu, B.; Abdalkarim, S.Y.H.; Li, Z.; Lu, W.; Yu, H.-Y. Synergistic Enhancement of High-Barrier Polylactic Acid Packaging Materials by Various Morphological Carbonized Cellulose Nanocrystals. *Carbohydr. Polym.* **2025**, *351*, 123118. [CrossRef]
19. Mahboub, N.; Cherfi, I.; Laouini, S.E.; Bouafia, A.; Benaissa, A.; Alia, K.; Alharthi, F.; Al-Essa, K.; Menaa, F. GC/MS and LC Composition Analysis of Essential Oil and Extracts from Wild Rosemary: Evaluation of Their Antioxidant, Antimicrobial, and Anti-Inflammatory Activities. *Biomed. Chromatogr.* **2025**, *39*, e70084. [CrossRef]
20. Yeddes, W.; Rybak, K.; Rebey, I.B.; Pietrzak, D.; Adamczak, L.; Hammami, M.; Wannes, W.A.; Witrowa-Rajchert, D.; Tounsi, M.S.; Tixier, A.S.F.; et al. Lipid Oxidation and Barrier Properties of the Coated Freeze-Dried Chicken Meat with Gelatin-Chitosan Film Enriched with Rosemary (*Rosmarinus officinalis* L.) Extract. *Foods* **2025**, *14*, 1127. [CrossRef]
21. Fard, G.C.; Parvinzadeh Gashti, M.; Dehdast, S.A.; Shabani, M.; Zarinabadi, E.; Seifi, N.; Berenjian, A. Novel Polyamide/Chitosan Nanofibers Containing Glucose Oxidase and Rosemary Extract: Fabrication and Antimicrobial Functionality. *Coatings* **2024**, *14*, 411. [CrossRef]
22. Ghasemian, S.O.; Ahmadi-Dastgerdi, A.; Abdollahi, A.; Tirtashi, F.E.; Zokaei, M.; Fallah, N.; NajafAbadi, P.I.; Dolatyari, F. The Effect of Active Packaging Film Based on Chitosan Containing Rosemary (*Rosmarinus officinalis* L.) Extract on Cheese Shelf Life. *J. Food Biochem.* **2024**, *2024*, 2108707. [CrossRef]
23. Jastaniah, S.D. Using Nisin-Chitosan Films Enriched with Rosemary Extract on *Listeria innocua*, *Escherichia coli* O157:H7 and *Pseudomonas aeruginosa* in Cold-Smoked Salmon during Cold Storage. *Appl. Food Res.* **2025**, *5*, 100693. [CrossRef]
24. Hoelscher, H.; Fell, E.L.; Colet, R.; Nascimento, L.H.; Backes, Â.S.; Backes, G.T.; Cansian, R.L.; Valduga, E.; Steffens, C. Antioxidant Activity of Rosemary Extract, Acerola Extract and a Mixture of Tocopherols in Sausage during Storage at 8 °C. *J. Food Sci. Technol.* **2024**, *61*, 69–83. [CrossRef]
25. Sahunie, A. Effect of *Rosmarinus officinalis* and *Origanum majorana* Extracts on Stability of Sunflower Oil during Storage and Repeated Heating. *Oil Crop Sci.* **2024**, *9*, 29–37. [CrossRef]
26. Giannakas, A.; Salmas, C.; Leontiou, A.; Tsimogiannis, D.; Oreopoulou, A.; Braouhli, J. Novel LDPE/Chitosan Rosemary and Melissa Extract Nanostructured Active Packaging Films. *Nanomaterials* **2019**, *9*, 1105. [CrossRef] [PubMed]
27. Mejía-Méndez, J.L.; Bach, H.; Lorenzo-Leal, A.C.; Navarro-López, D.E.; López-Mena, E.R.; Hernández, L.R.; Sánchez-Arreola, E. Biological Activities and Chemical Profiles of Kalanchoe Fedtschenkoi Extracts. *Plants* **2023**, *12*, 1943. [CrossRef] [PubMed]

28. García-Betanzos, C.I.; Hernández-Sánchez, H.; Bernal-Couoh, T.F.; Quintanar-Guerrero, D.; Zambrano-Zaragoza, M.d.l.L. Physicochemical, Total Phenols and Pectin Methylesterase Changes on Quality Maintenance on Guava Fruit (*Psidium guajava* L.) Coated with Candeuba Wax Solid Lipid Nanoparticles-Xanthan Gum. *Food Res. Int.* **2017**, *101*, 218–227. [CrossRef]
29. Dhiman, S.; Kumari, A.; Kumari, S.; Sharma, R. Advanced Biodegradable Starch-Based Nanocomposite Films Incorporating Zinc Oxide Nanoparticles: Synthesis, Characterization, and Efficacy in Antibacterial Food Packaging Applications. *J. Environ. Chem. Eng.* **2025**, *13*, 116296. [CrossRef]
30. Shah, S.; Oh, J.; Bang, Y.; Jung, S.; Kim, H.-C.; Jeong, K.S.; Park, M.H.; Lee, K.A.; Ryoo, J.-H.; Kim, Y.-J.; et al. Pregnant Women's Lifestyles and Exposure to Endocrine-Disrupting Chemicals: A Machine Learning Approach. *Environ. Pollut.* **2025**, *366*, 125309. [CrossRef]
31. Wyrwisz, J.; Moczkowska-Wyrwisz, M.; Kurek, M.A. Development of Modified Gas Composition for Atmosphere Packaging of Sliced Apple Chips. *Appl. Sci.* **2025**, *15*, 2832. [CrossRef]
32. Karaogul, E.; Ugurtay, A.; Kelley, S.S.; Alma, M.H. Modelling on Extractions and Micro Nano Encapsulation of Pistacia Terebintus Cambium Layer Gum Essential Oil; Antioxidant Activity and Structural Approach Via XRD, SEM and TGA/DSC. *Plant Foods Hum. Nutr.* **2025**, *80*, 57. [CrossRef] [PubMed]
33. Huerta-Vera, K.; Flores-Andrade, E.; Arévalo-Galarza, M.d.L.C.; Cadena-Iñiguez, J.; Castillo-Morales, M.; Vivar-Vera, G.; Jiménez-Guzmán, J.; Soto-Hernández, R.M. Optimal Storage Conditions for Spray-Dried Chayote Juice (*Sechium edule* (Jacq.) Sw. Cv. Perla Negra) Microencapsulated with Gum Arabic. *Food Bioprod. Process.* **2025**, *150*, 296–309. [CrossRef]
34. Gómez-Gaete, C.; Avendaño-Godoy, J.; Escobar-Avello, D.; Campos-Requena, V.H.; Rogel-Castillo, C.; Estevinho, L.M.; Martorell, M.; Sharifi-Rad, J.; Calina, D. Revolutionizing Fruit Juice: Exploring Encapsulation Techniques for Bioactive Compounds and Their Impact on Nutrition, Flavour and Shelf Life. *Food Prod. Process Nutr.* **2024**, *6*, 8. [CrossRef]
35. Kamalpour, R.; Koocheki, A.; Ghorani, B. Encapsulation of D-Limonene in *Lepidium perfoliatum* Seed Gum/PVA Electrospun Nanofibers: Physicochemical Characterization and Modeling the Kinetics of Release. *Curr. Res. Food Sci.* **2025**, *10*, 100966. [CrossRef]
36. Guo, Z.; Ren, J.; Song, C. Enhanced Thermal and Storage Stability of Glucose Oxidase via Encapsulation in Chitosan-Coated Alginate and Carboxymethyl Cellulose Gel Particles. *Foods* **2025**, *14*, 664. [CrossRef]
37. Sattari, A.; Basirattalab, A.; Alemzadeh, I. Fabrication of pH-Sensitive Bacterial Cellulose/Carboxymethyl Cellulose Hybrid Hydrogel Beads in Agitated Culture for Oral Drug Delivery. *Can. J. Chem. Eng.* **2025**, *203*, 3521–3530. [CrossRef]
38. Siddiqui, S.A.; Singh, S.; Bahmid, N.A.; Mehany, T.; Shyu, D.J.H.; Assadpour, E.; Malekjani, N.; Castro-Muñoz, R.; Jafari, S.M. Release of Encapsulated Bioactive Compounds from Active Packaging/Coating Materials and Its Modeling: A Systematic Review. *Colloids Interfaces* **2023**, *7*, 25. [CrossRef]
39. Abdullah; Cai, J.; Hafeez, M.A.; Wang, Q.; Farooq, S.; Huang, Q.; Tian, W.; Xiao, J. Biopolymer-Based Functional Films for Packaging Applications: A Review. *Front. Nutr.* **2022**, *9*, 1000116. [CrossRef]
40. Maphosa, B.; Tsige, A.A.; Van Breda, V.; Caleb, O.J.; Opara, U.L. Investigating the Effects of Pre-Treatment, Drying Techniques and Packaging on Nutritional Quality and Shelf-Life of Pomegranate Arils. *LWT* **2025**, *215*, 117240. [CrossRef]
41. Panthi, K.P.; Shahi, D.K.; Sharma, M.L.; Li, Z.; Pandey, L.M.; Joshi, M.K. Gluten-Based Composite Film for Smart Food Packaging Applications. *Food Bioprocess. Technol.* **2025**, *18*, 2882–2898. [CrossRef]
42. Yang, L.; Yuan, F.; Zhou, M.; Zhou, X.; Ahmmed, M.K.; Wu, H. Insights into Low-Temperature Strategies for Preserving Cooked Pork Quality in Ready-to-Eat Meat Products through Processing and Reheating Studies. *Food Chem.* **2025**, *487*, 144696. [CrossRef] [PubMed]
43. Lee, I.; Lee, J.; Kim, M. Inhibition of *Salmonella* Growth in Exudates Drained from Poultry Meat by Bacteriophage Cocktail-Containing Absorbent Food Pad. *LWT* **2024**, *197*, 115908. [CrossRef]
44. Li, Z.; He, Q.; Lai, J.; Lin, J.; Wu, S.; Guo, Z.; Zheng, H. Effect of Stepwise Cooking on the Water-Retention Capacity and Protein Denaturation Degree of Chicken Breast. *Int. J. Gastron. Food Sci.* **2024**, *38*, 101012. [CrossRef]
45. Xu, S.; Falsafi, S.R. Juiciness of Meat, Meat Products, and Meat Analogues: Definition, Evaluation Methods, and Influencing Factors. *Food Rev. Int.* **2024**, *40*, 2344–2377. [CrossRef]
46. Wang, B.; Wang, S.; Xu, Y.; Jiang, Q.; Xia, W. Colour Stability Improving of Yellowfin Tuna Slices by Compound Antioxidant against Oxidation of Myoglobin. *Int. J. Food Sci. Technol.* **2024**, *59*, 5616–5629. [CrossRef]
47. Bueno, L.O.; Massingue, A.A.; Ramos, A.d.L.S.; Ferreira, D.D.; Ramos, E.M. Meat Color by Numbers: Evaluation of the Myoglobin Redox Forms by Different Methods and Its Relationship to CIE Color Indices. *J. Food Compos. Anal.* **2024**, *133*, 106365. [CrossRef]
48. Orkusz, A.; Rampanti, G.; Michalczuk, M.; Orkusz, M.; Foligni, R. Impact of Refrigerated Storage on Microbial Growth, Color Stability, and pH of Turkey Thigh Muscles. *Microorganisms* **2024**, *12*, 1114. [CrossRef]
49. Liao, Z.; Parumasivam, T.; Zhu, X.; Tan, T.-C. Selected Medium-Chain Dicarboxylic Acid Combinations: Improving the Shelf Life and Quality of Beef During Chilled Storage. *Food Bioprocess. Technol.* **2025**, *18*, 3521–3537. [CrossRef]

50. Lee, Y.Y.; Lee, S.; Ham, S.H.; Lee, M.G.; Hahn, J.; Kim, Y.; Choi, Y.J. Relationship between Sensory Attributes and Instrumental Texture Properties in Meat Analog Patty System Substituted with Sweet Potato Stem. *J. Sci. Food Agric.* **2024**, *104*, 7002–7012. [CrossRef]
51. Hao, D.; Tu, X.; Zhang, X.; Guo, S.; Sun, L.; Li, J.; Wang, D.; Xu, W.; Li, P. Effects of Proteases Inactivation on Textural Quality of Yellow-Feathered Chicken Meat and the Possible Mechanism Based on Myofibrillar Protein. *Food Control* **2024**, *166*, 110713. [CrossRef]

Disclaimer/Publisher's Note: The statements, opinions and data contained in all publications are solely those of the individual author(s) and contributor(s) and not of MDPI and/or the editor(s). MDPI and/or the editor(s) disclaim responsibility for any injury to people or property resulting from any ideas, methods, instructions or products referred to in the content.